

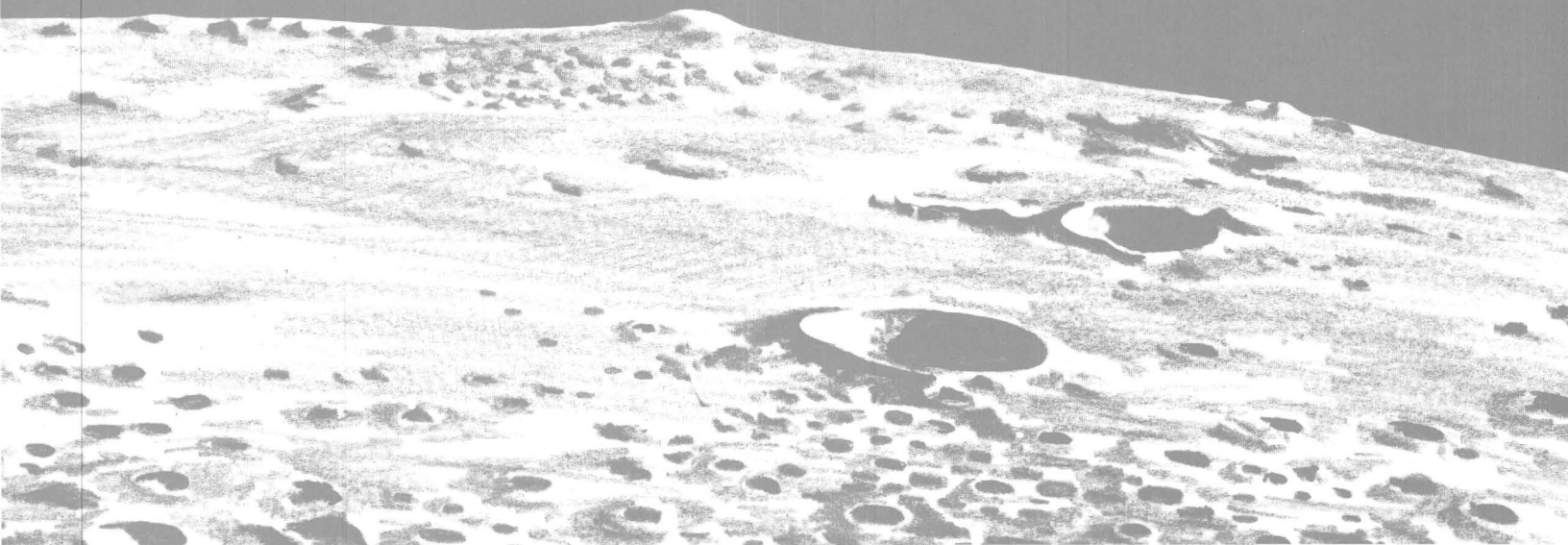
# SEISMIC DETECTION OF NEAR-SURFACE CAVITIES

## CONTRIBUTIONS TO ASTROGEOLOGY

Prepared on behalf of the National Aeronautics and Space Administration



GEOLOGICAL SURVEY PROFESSIONAL PAPER 599-A





# Seismic Detection of Near-Surface Cavities

By JOEL S. WATKINS, RICHARD H. GODSON, *and* KENNETH WATSON

CONTRIBUTIONS TO ASTROGEOLOGY

---

GEOLOGICAL SURVEY PROFESSIONAL PAPER 599-A

*Prepared on behalf of the  
National Aeronautics and Space Administration*



**UNITED STATES DEPARTMENT OF THE INTERIOR**

**STEWART L. UDALL, *Secretary***

**GEOLOGICAL SURVEY**

**William T. Pecora, *Director***

## CONTRIBUTIONS TO ASTROGEOLOGY

Astrogeology is the study of the earth as a planetary body, especially as a member of a family of planetary bodies and of the solar system. The viewpoint of the discipline of astrogeology thus lies between the traditional viewpoint of geology and that of planetary astronomy. The methods of research in astrogeology include classical methods of geology and astronomy as well as new methods that have been developed in this new field.

The principal goal of research in astrogeology is the solution of several cardinal problems of geology. Solution of these problems is sought primarily through comparison of the earth with the moon and other terrestrial planets, particularly from the standpoint of the earth as a member of a double-planet system—the earth-moon system. Outstanding among the geologic problems amenable to attack by this comparison are (1) the origin and early history of the earth-moon system, (2) the internal composition of the earth and the moon, and (3) the nature and mechanisms of the principal processes that have governed the geologic evolution of the earth and the moon.

The U.S. Geological Survey's planned program of research in astrogeology includes (1) basic studies of the history of the earth-moon system, the chemistry and petrology of lunar and planetary materials, and the physics and major geologic processes of planets, and (2) participation in the scientific aspects of the lunar and planetary exploration programs of the National Aeronautics and Space Administration. Among the specific topics currently under study in the basic research program are the morphology, stratigraphy, structure, and geologic history of the moon; the chemistry and petrology of meteorites, tektites, and cosmic dust; the geologic record of infall of cosmic material on the earth; the distribution in space and time of bodies of subplanetary dimensions in the solar system and their rate of encounter with the earth and the moon; the physics of impact and its effects as a geologic process on the earth and the moon; the emission and scattering of radiation from planetary surfaces; and the heat budget of the earth and the moon. Members of the Geological Survey staff have participated or are currently participating in the Luster, Gemini, Ranger, Surveyor, Lunar Orbiter, and Apollo flight projects of the NASA. This work includes development of instruments and techniques for use in space, on the lunar surface, and in postflight reduction of returned photographic and other data; scientific analysis of returned data needed during operation of the space-flight missions; and detailed postflight analysis and interpretation of the data on cosmic dust and data on the lunar surface acquired from the space-flight missions.

Since the start of the program in 1960, the results of the Geological Survey research in astrogeology have appeared in preliminary or final form in a variety of books, journals, and map series and in numerous informal publications not readily obtainable by the public. The present volume is the first of a series of professional papers that will describe major results of research in astrogeology.

EUGENE M. SHOEMAKER.



## CONTENTS

	Page		Page
Abstract.....	A1	Field studies.....	A4
Introduction.....	1	Signal enhancement.....	7
Methods of detection.....	2	Summary.....	12
Free oscillations.....	2	References.....	12
Anomalous amplitude attenuations.....	4		
Delays in arrival times.....	4		

## ILLUSTRATIONS

		Page
FIGURE 1.	Photograph of part of the Rima Hyginus.....	A1
2.	Photograph of part of the crater Alphonsus obtained by Ranger IX.....	2
3.	Photograph of collapsed section of roof of a lava tunnel in the Pisgah lava flow, San Bernardino County, Calif.....	3
4.	Photograph of interior of a lava tunnel in the Pisgah lava flow, San Bernardino County, Calif.....	3
5.	Graph showing group-velocity curves for an empty cylindrical hole.....	3
6.	Part of a seismogram recorded over a lava tunnel in the Pisgah lava flow, San Bernardino County, Calif.....	4
7.	Graph showing amplitudes of first-arriving seismic energy recorded over a lava tunnel in the Kana-a lava flow, Coconino County, Ariz.....	5
8.	Plan and profiles of a lava tunnel in the Pisgah lava flow, San Bernardino County, Calif.....	6
9.	Section showing geology of the U4B nuclear shot point and vicinity and locations of seismic lines, Nevada Test Site, north of Mercury, Nev.....	7
10.	Composite seismogram recorded at the U4B nuclear shot point, from chemical explosions north of the seismic lines.....	8
11.	Replay of tape 39179 showing delays in events B and C in the vicinity of the U4B shot point.....	9
12.	Graph showing ratio of observed amplitudes of first-arriving seismic energy recorded in the vicinity of the U4B shot point to an empirical amplitude function.....	9
13.	Part of a seismogram recorded over the cavity at the U4B shot point showing attenuation of amplitudes of first-arriving energy from the south shot point.....	10
14.	Graphs showing amplitude spectra calculated for selected seismic recordings.....	11
15.	Graph showing autocorrelation function for selected seismic recordings over and adjacent to Pisgah lava tunnel, San Bernardino County, Calif.....	12

## TABLE

		Page
TABLE 1.	Cavity statistics.....	A12





## CONTRIBUTIONS TO ASTROGEOLOGY

### SEISMIC DETECTION OF NEAR-SURFACE CAVITIES

By JOEL S. WATKINS, RICHARD H. GODSON, and  
KENNETH WATSON

#### Abstract

Oscillations with durations of 1 second or more and with narrow frequency bands have been observed over cavities in lava and alluvium at depths ranging from 1 to 14 meters. They are probably primarily radial oscillations of cavity walls, and calculations show that dominant frequencies are generally within a factor of 3 of those computed from M. A. Biot's theoretical results for radial oscillations of a cylindrical hole in an infinite solid.

Delays in arrival times and anomalous attenuation of seismic waves traversing cavities have also been observed. Fractured and broken rock in the chimney above a nuclear explosion cavity is thought to be responsible for delays in Rayleigh waves and delays in what are probably trapped waves.

Fourier analysis and autocorrelation have been used successfully to detect these and similar resonant phenomena in noisy backgrounds; crosscorrelation of proximate traces was less successful for this purpose.

#### INTRODUCTION

Much evidence indicates that volcanism is a significant contributor to lunar morphologic features and geology. Prominent examples of probable lunar volcanic structures include the dimple craters seen in the Ranger VIII photography (N. J. Trask, oral commun., 1965), linear chains of craters of the Rima Hyginus (fig. 1), and rilles and associated craters of the Alphonsus region shown in Ranger IX photographs (fig. 2). The rilles and craters of the Alphonsus region are probably analogous to the Chain of Craters in Hawaii.

Lava tunnels, common and widespread in many terrestrial basaltic lava flows (figs. 3, 4), also may occur on the moon because parts of the mare surface apparently consist of lava flows.

Lunar lava tunnels, if they exist, might facilitate exploration by sheltering astronauts and their equipment during meteorite showers or intensive solar radiation. Such tunnels might be cold traps where ice has accumulated (Watson and others, 1961) and would thus be of further use. On the other hand, tun-

nels with thin roofs, such as the one shown in figure 3, would endanger lunar explorers. For these reasons, astronauts may require a technique for detection of near-surface cavities on the moon. Such a technique, employing seismic principles, has already been used at a Wyoming damsite and is the subject of this report.

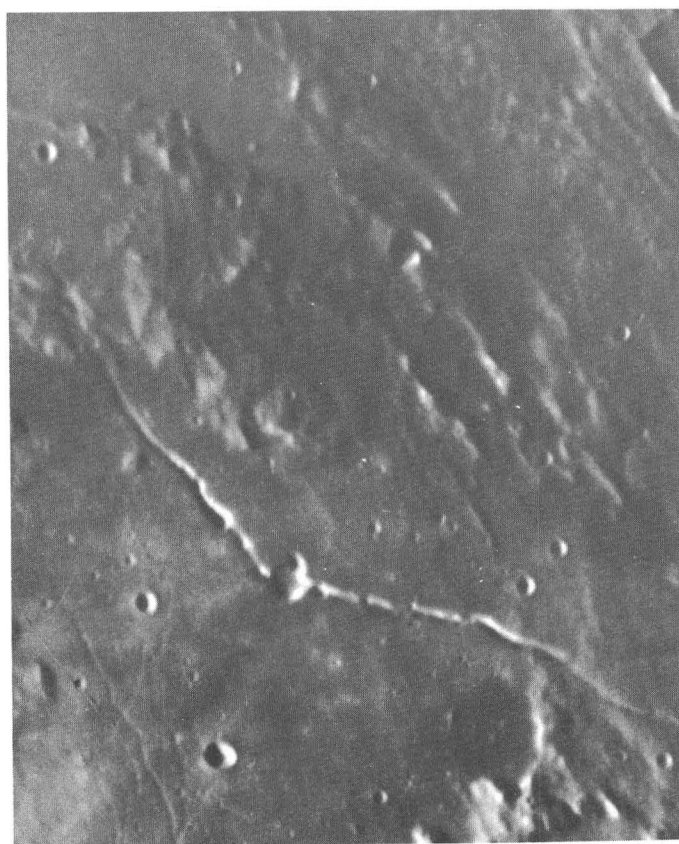


FIGURE 1.—Part of the Rima Hyginus. Craters along the rima may be collapse structures. Largest crater on the rima is about 11 kilometers in diameter. Photograph taken at Pic du Midi Observatory, France.

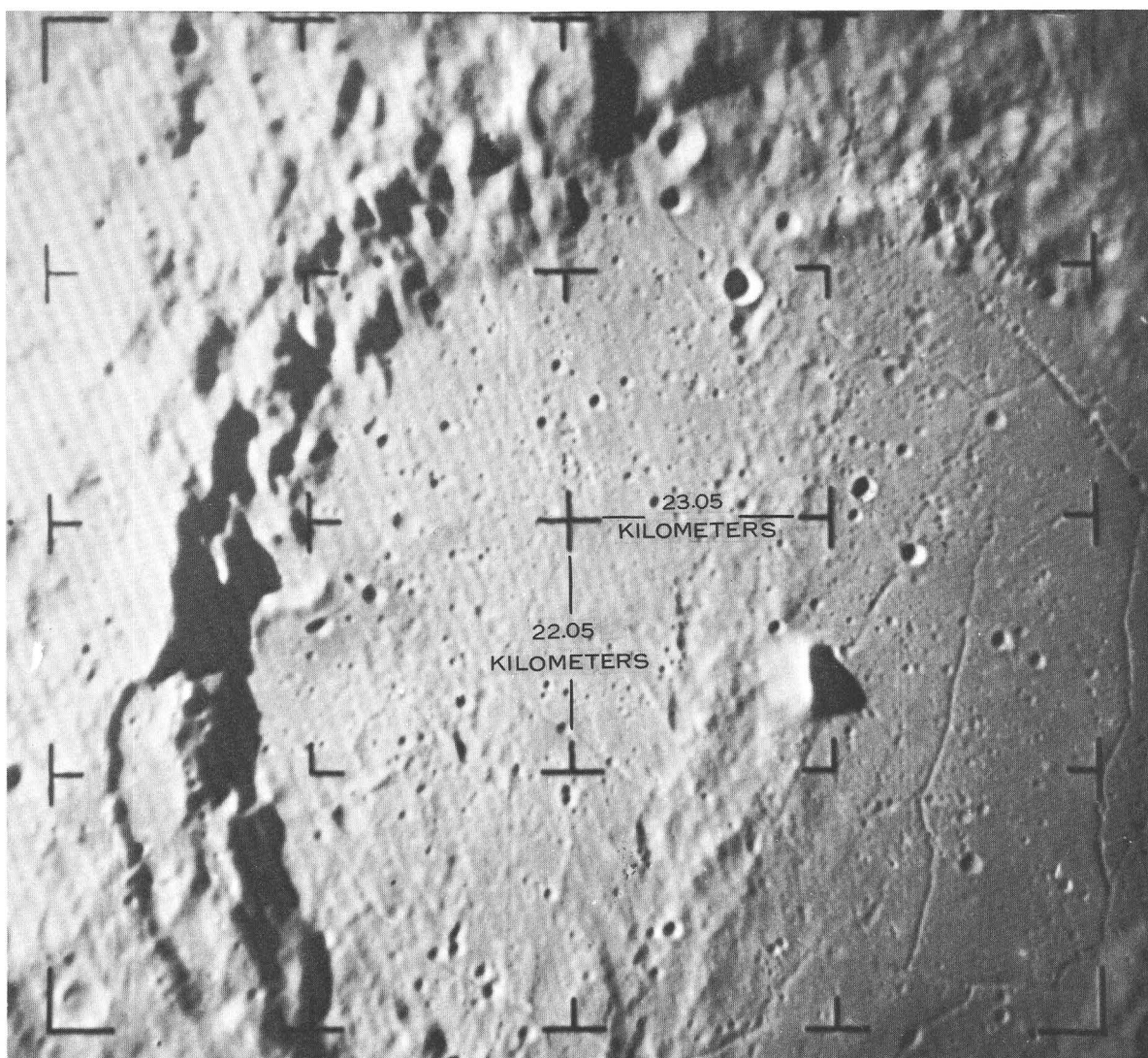


FIGURE 2.—Part of the crater Alphonsus shown by Ranger IX photograph (Jet Propulsion Laboratory, 1966). Many rilles have conspicuous associated craters which may be collapse craters. Scale shown is approximate.

#### METHODS OF DETECTION

The U.S. Geological Survey, on behalf of the Manned Spacecraft Center, National Aeronautics and Space Administration, has been examining seismic characteristics of certain types of terrestrial near-surface rocks. Lavas and pyroclastic materials, because they are thought to be analogous to lunar near-surface materials, received the most attention. Seismic studies conducted over lava tunnels indicated that tunnels can be located and their approximate size determined by seismic techniques. Results of studies in the vicinity of the U4B nuclear cavity at the Nevada Test Site confirmed this.

Three seismic phenomena—free oscillations of the cavity walls, anomalous amplitude attenuations, and delays in arrival times—have provided evidence of

cavities or of associated adjacent brecciated zones. Of these, the first appears to be most diagnostic for location and delineation of cavities. The second and third may provide significant supplemental data.

#### FREE OSCILLATIONS

Main characteristics of cavity oscillations can be treated most simply by examining the period equation for relatively simple geometric shapes. Biot (1952) computed the period equation for radial oscillations of a cylindrical hole in an infinite solid. Resultant group-velocity curves for a variety of elastic solids (with Poisson's ratio ranging from 0 to 0.50) indicate that the minimum dispersion occurs at wavelengths approximately 1.5 times the cavity diameter (see fig. 5).

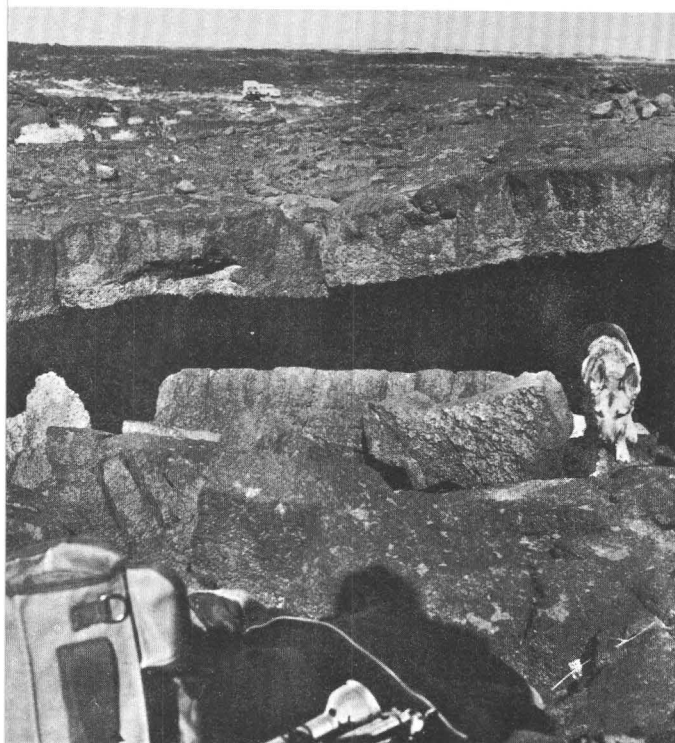


FIGURE 3.—Collapsed section of roof of a lava tunnel in the Pisgah lava flow, San Bernardino County, Calif.

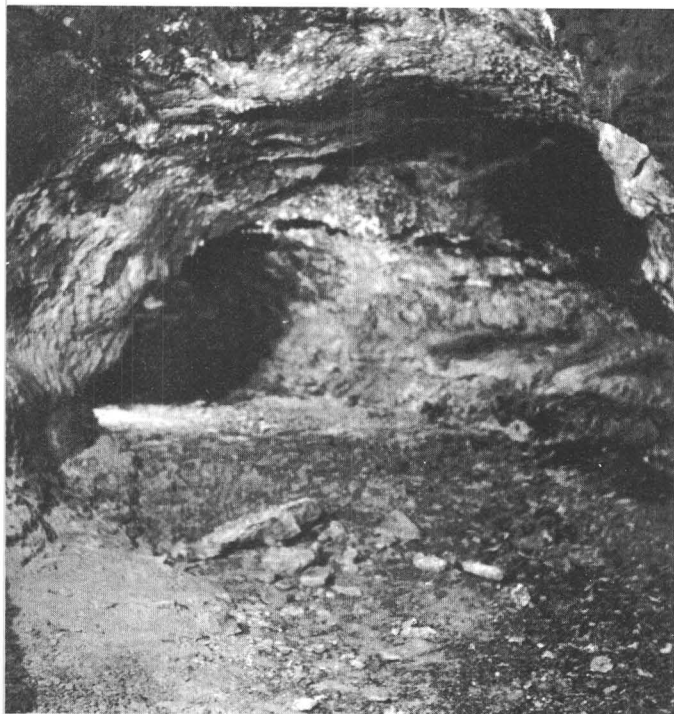


FIGURE 4.—Interior of a lava tunnel in the Pisgah lava flow, San Bernardino County, Calif.

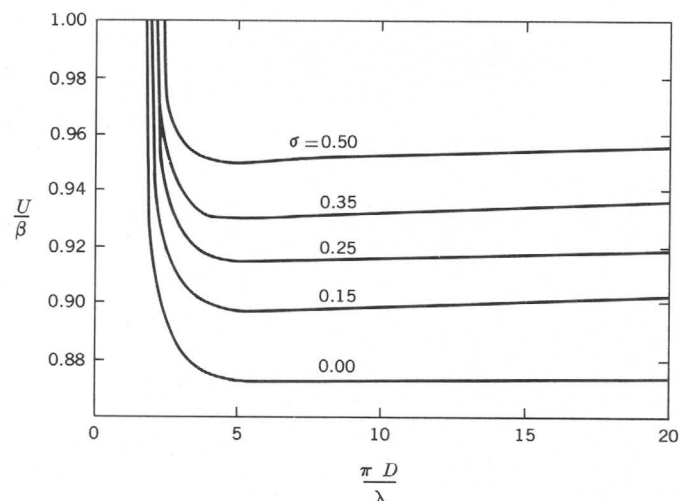


FIGURE 5.—Group-velocity curves for an empty cylindrical hole (after Biot, 1952) where  $D$  is the hole diameter;  $\beta$ , the shear velocity of the surrounding space;  $U$ , the group velocity;  $\lambda$ , the wavelength; and  $\sigma$ , Poisson's ratio.

The radiation field about a cavity can be visualized as the response of a tuned circuit with a finite resistance. The more rapid the energy loss due to radiation, the lower the  $Q$  of the circuit and the wider the frequency spectrum of radiation from it. In order to maintain the resonant frequency with a narrow bandwidth, the circuit must be driven with a harmonic source of that frequency.

In the field, oscillations have been excited in cavity walls by waves from an explosion near ground surface. The seismic energy spectrum is sufficiently broad to induce oscillations in walls of cavities whose diameters range from a few meters to several tens of meters.

Oscillations propagate through rock to the surface where they are sensed by conventional seismometers, amplified, and recorded on the seismograph. Wall oscillations persist much longer than the initial ground motion and have been recorded for as long as 4 seconds after the explosion.

Figure 6 shows high-amplitude resonant oscillations recorded over a lava tunnel. Three groups of geophones, eight in each group, were arrayed linearly transverse to the tunnel. One group was approximately over the tunnel; the other two, outside the tunnel walls. The oscillations, which were recorded most intensely by the central group, are similar to those recorded over two other near-surface cavities that were studied.



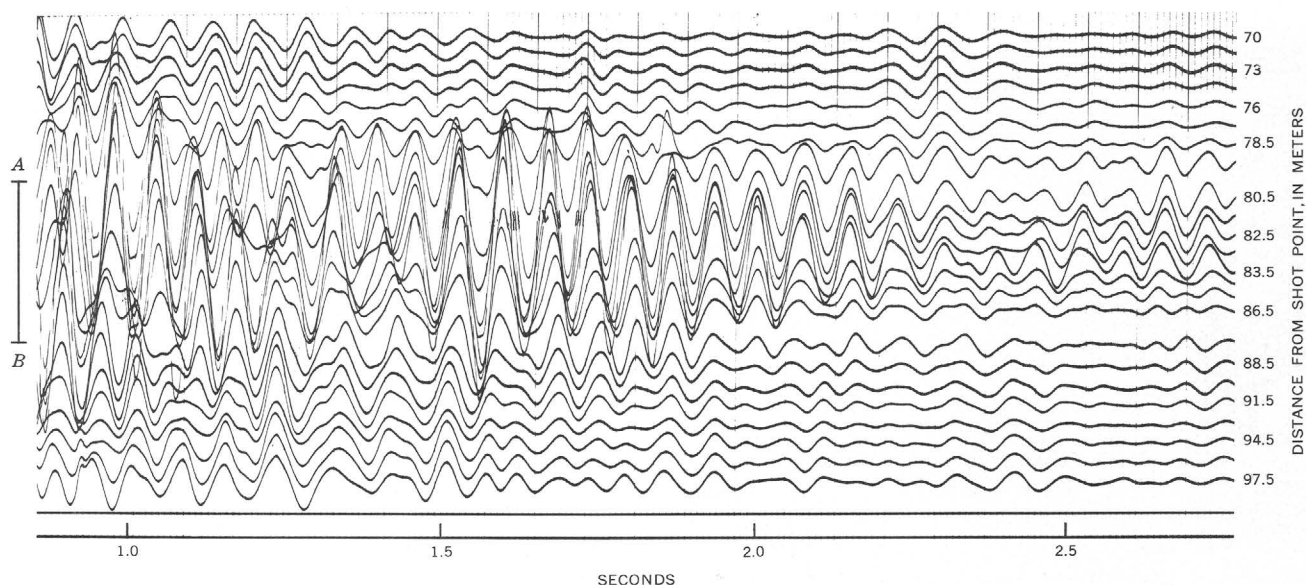


FIGURE 6.—Part of a seismogram recorded over a lava tunnel in the Pisgah lava flow, San Bernardino County, Calif. Note prominent in-phase cavity oscillations in center of seismogram. *AB* indicates the location and approximate width of the tunnel.

Note in figure 6 that the dominant frequency is relatively uniform with time. This characteristic of wall oscillations suggests that they can be identified by correlation techniques when oscillation amplitudes are much lower than the total amplitude spectrum of random noise in the area.

Multiple geophone and multiple shot-point configurations, which are common in reflection seismology, may be useful in signal-to-noise enhancement of wall oscillations.

#### ANOMALOUS AMPLITUDE ATTENUATIONS

Variations of amplitude attenuation in unconsolidated or semiconsolidated lunar analog materials are primarily caused by energy absorption during inelastic movement of uncemented or poorly cemented rock particles and by reflection and diffraction from joints and fractures in the rocks. Decreased cementation or increased jointing or fracturing results in increased attenuation of amplitudes of waves traversing the material.

Amplitudes of waves passing by a cavity will generally decrease as a result of reflection at the cavity, conversion of part of the energy to wall oscillations, and scattering in the fractured zone adjacent to a nuclear cavity or in the chimney above such a cavity. Amplitudes of reflected waves have been successfully used (Cook, 1965) to delineate solution cavities in salt beds, and anomalous reflection amplitudes over lava tunnels have been observed in the present studies.

Refracted waves traversing cavities and adjacent fractured and collapsed zones can be generated in most areas because velocity increases with depth. Surface waves and shear waves may also show anomalous amplitude variations in the vicinity of a cavity, a chimney, or a jointed zone. Additional studies are required to evaluate the usefulness of these arrivals.

Rocks above the focus of a nuclear explosion are visibly fractured, and the fractures should attenuate amplitudes of direct arrivals from nearby shot points which horizontally traverse the fracture zone.

#### DELAYS IN ARRIVAL TIMES

A wave front traversing a shallow cavity may exhibit a measurable delay in the lee of the cavity, but wave paths exist in the vicinity of deep cavities along which energy can propagate with insignificant travel-time delays. Delays of arrival times are most evident where cavities are near the surface or where large chimneys overlie nuclear cavities. The nearer a chimney top is to ground surface, the easier is identification of delays in arrival of direct, refracted, reflected, and surface waves. If a high chimney is not present, waves reflected from a discontinuity below the cavity probably offer the best possibility of success in exhibiting a time delay.

#### FIELD STUDIES

Initial studies were conducted over a small lava tunnel in the Kana-a lava flow about 24 kilometers northeast of Flagstaff, Ariz. The top of the tunnel is

approximately 1.5 meters beneath the surface of the ground; the diameter is between 2 and 3 m. The Kana-a flow comprises two layers of basaltic lava: an upper layer consisting of scoriaceous, vesicular, and fractured aa basalt and a lower layer of hard dense sparsely vesicular basalt at depths ranging from 1.5 to 4.5 m below the surface of the flow. The average compressional-wave velocity is approximately 800 mps (meters per second), and the average shear-wave velocity is approximately 450 mps.

A linear array of 24 geophones was laid perpendicular to and centered over the longitudinal axis of the tunnels. Shots of varying sizes were detonated along the seismic array and along the projection of the array at distances ranging from 0 to 85 m from the axis of the tunnel. A pronounced anomaly in amplitudes of waves refracted through the dense lava at the base of the flow from a shot 85 m from the axis of the tunnel was observed directly over the tunnel and for a short distance along the seismic array on the side of the tunnel away from the shot point. (See fig. 7.)

Small variations in amplitudes of reflected waves from horizons below the tunnel also were observed. A small delay was also noted in arrival times of the reflections, but the noise level made it difficult to define the delay with precision. No delays were observed in the refracted arrivals.

Cavity oscillations were not immediately identified on the Kana-a records. The dominant frequency of the oscillations, about 34 cps (cycles per second), is nearly the same as that of reflections recorded in the area. Hence, oscillations were not as obvious there as they were in areas where wall oscillation frequencies differed significantly from other seismic signals.

The next experiments were conducted in much the same manner over a lava tunnel in the Pigsaw flow in the Mohave Desert of southern California. This basalt flow is adjacent to and south of U.S. Highway 66, about 60 km east of Barstow, Calif. The flow surface is characterized by roughly equal areas of aa and pahoehoe lava. The tunnel, which is in the area of pahoehoe, was traced at least 1.1 km northward from the base of the Pigsaw cinder cone. Figure 8 shows a plan, profiles, and spread locations in the part of the tunnel that was investigated.

Wall oscillation waves were first recognized during the study at the Pigsaw site, and procedures for inducing strong oscillations were developed. Shots fired several tens of meters away and buried 0.3 to 0.1 m in holes hacked out of the lava had enough energy at the proper frequency to induce strong waves in the cavity. Figure 6 is a record of cavity oscillations at

the Pigsaw tunnel. The compressional-wave velocity measured in this lava was 1,100 mps; shear-wave velocities have not yet been measured but were probably about 650 mps.

The third area of investigation was centered about the shot point for nuclear explosion U4B in Yucca Valley at the Atomic Energy Commission's Nevada Test Site. The U4B shot consisted of a low-yield nuclear device placed approximately 440 m below the surface of the ground. The explosion created a chimney that extends upward to within 25 m of the surface. Postshot drilling revealed an open cavity at least 14 m high. The exact diameter of the cavity is unknown but is estimated to be at least 30 m (F. N. Houser, oral commun., 1965). (See fig. 9.) Data were obtained from three seismic spreads of 24 detectors, each spread spaced at intervals of 10 m. Three detectors were overlapped on adjacent spreads in order to normalize amplitude variations caused by different shothole conditions. Data from these spreads were composited, and a composite record showing energy received from the north end of the array is shown in figure 10.

Cavity oscillations shown in figure 10 are not as coherent as those in figure 6 but are easily identifiable between 460 and 520 m from the north end. The earlier, noisier part of the record suggests that high-amplitude waves are present and that correlation techniques could enhance signal-to-noise ratios.

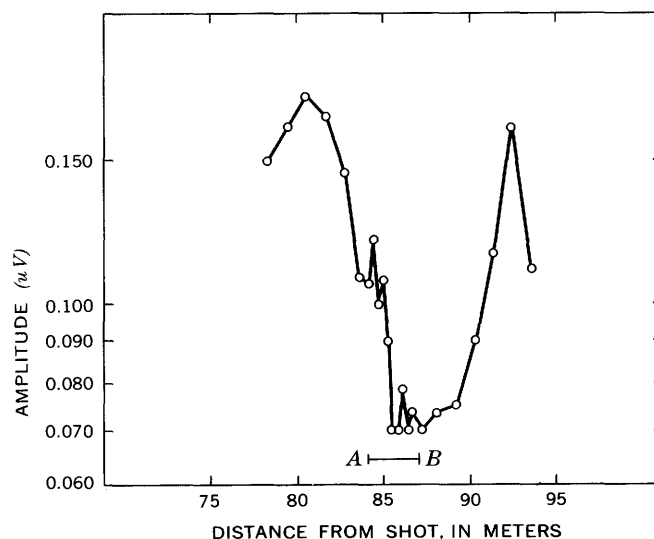


FIGURE 7.—Amplitudes of first arriving seismic energy recorded over a lava tunnel in the Kana-a lava flow near Flagstaff, Coconino County, Ariz. Dip of the emerging wave front causes the amplitude anomaly to be most pronounced on the side of the tunnel away from the shot. AB indicates the approximate location and width of the tunnel.

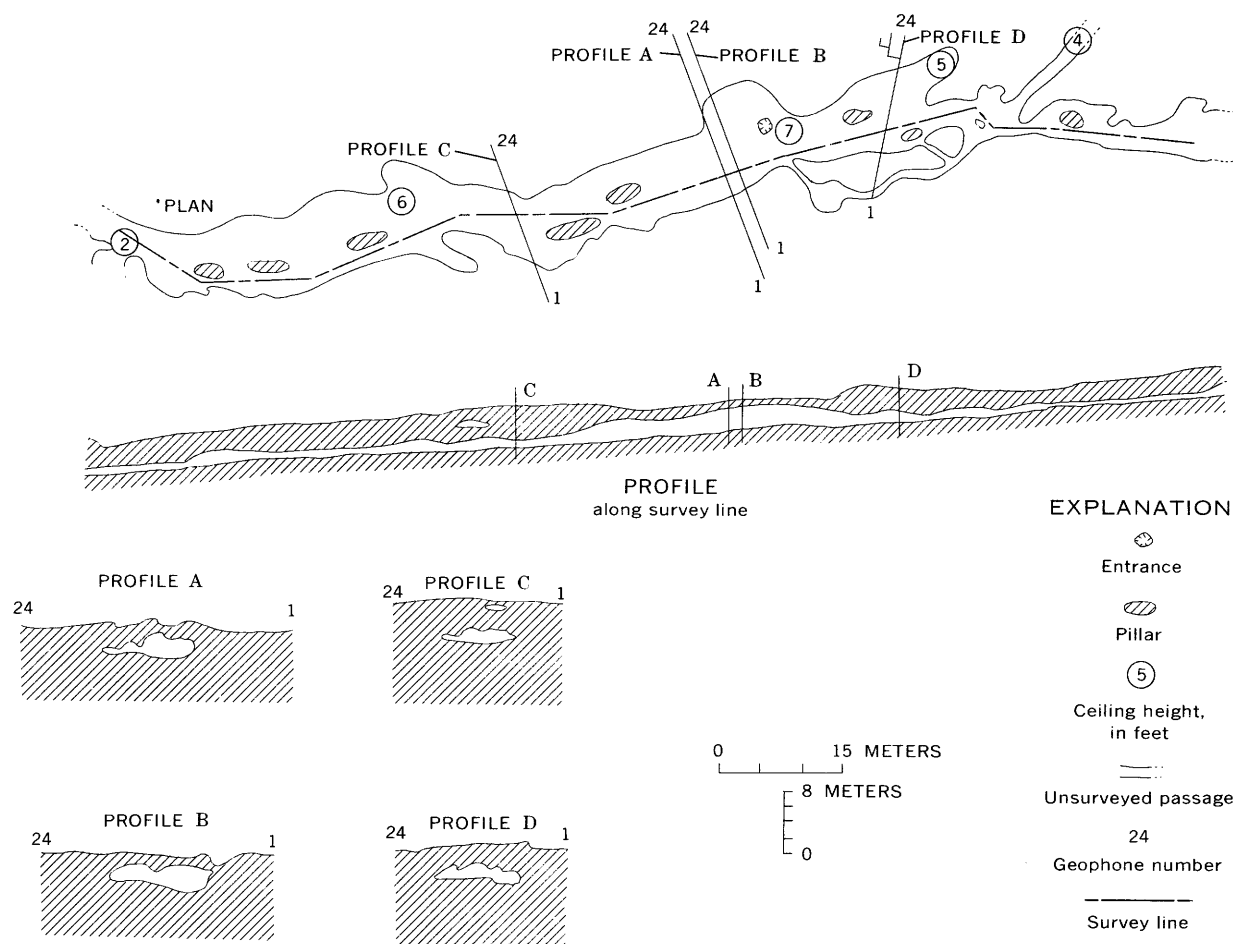


FIGURE 8.—Plan and profiles of a lava tunnel in the Pisgah lava flow, San Bernardino County, Calif. Surveyed by transit and tape.

Two pronounced later events are indicated in figure 11 by one darkened trough of each event. (Fig. 11 is a replay of the middle record of fig. 10. The time base and filtering were varied in order to improve resolution of wall oscillations in fig. 10 and of later events in fig. 11.) In figure 11 event C is thought to be the Rayleigh wave. The cause of event B is not entirely clear; however, event B may be a trapped wave in a low-velocity layer within the alluvium.

Although arrival times of the head wave show no anomalies in the vicinity of the cavity, arrival times of both events B and C are delayed in the vicinity of the cavity, which suggests that first-arriving energy traveled in the solid material above the cavity but that significant energy of events B and C traveled at deeper levels and traversed either the cavity or the chimney. The width of the zone in which the delay occurred probably equals the greatest width of the chimney.

Examination of amplitudes of first arrivals (figs.

12, 13) shows an anomalous decrease over the cavity and for a short distance on the side of the cavity away from the shot.

The empirical method used to reduce data shown in figure 12 was as follows: Data were normalized for shot-point variations by use of an amplitude function,  $A_e = ae^{-bd}$  ( $A_e$ =amplitude,  $d$ =distance from shot point, and  $a$  and  $b$  are arbitrary constants).  $A$  and  $b$  were determined by a least-squares solution for the equation,  $y = mx + c$ , where  $y = \ln A_e$ ,  $x = d$ ,  $m = -b$ , and  $c = \ln a$ . The ratio  $A_e/A_o$  ( $A_o$ =observed amplitude) was computed for each point and plotted as shown in figure 12.

Data in figure 12 show that amplitudes directly over the nuclear focus and on the sides of the nuclear focus opposite shot points are reduced by as much as an order of magnitude relative to the empirical function. A slight asymmetry with respect to the epicenter suggests that the axis of the cone of fractured material above the focus is inclined slightly to the north.

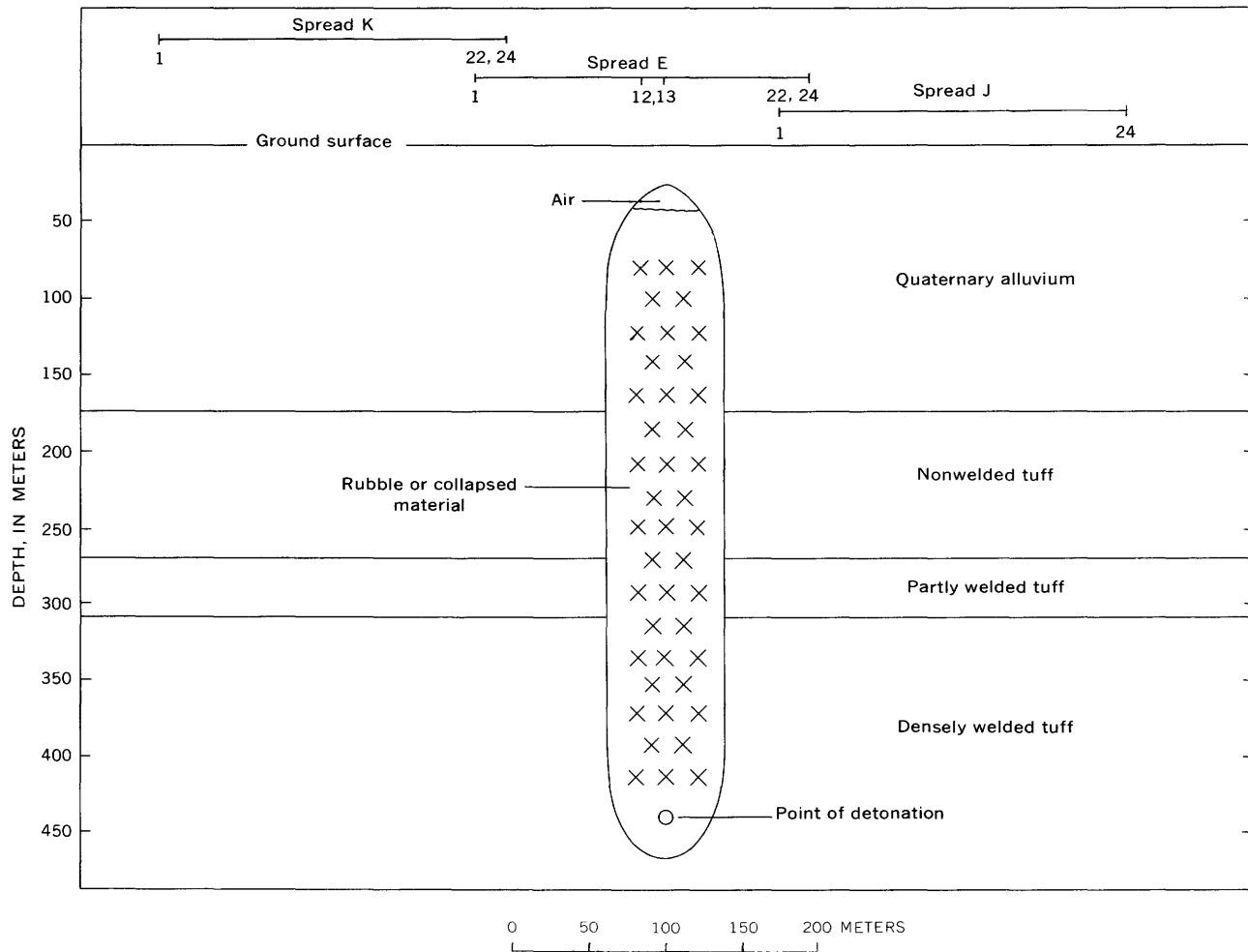


FIGURE 9.—Geology of the U4B nuclear shot point and vicinity and locations of seismic lines, Nevada Test Site, north of Mercury, Nev.

No noise-canceling seismometer arrays or shooting patterns were attempted, although previous investigators in Yucca Valley have significantly enhanced signal-to-noise ratios of reflection data with these techniques (R. M. Hazlewood, oral commun., 1965).

#### SIGNAL ENHANCEMENT

The relatively long duration and narrow frequency band of cavity oscillations suggest three methods of signal enhancement, each offering the possibility of identifying cavity oscillations despite a noisy background. The simplest technique is a Fourier analysis of a selected window in the record. The magnitude of the spectrum for a specific frequency is proportional to the average amplitude of the wave energy at that frequency in the selected window. Consequently, a longer duration of the cavity oscillations will yield a larger spectrum than the spectra for some

transient waves, even though individual amplitude peaks of the transients may be larger than the mean amplitude of the cavity oscillation. Cavity oscillations that exhibit significant higher modes of vibration can be detected by examination of the spectrum.

The autocorrelation function can also serve as a means of locating weak signals of long duration in a noisy background. The dominant frequency can be estimated from the frequency of the autocorrelation function.

If it is assumed that the cavity radiates a signal with a distinctive signature which is received at all geophones, the crosscorrelation function for two proximate geophones over the cavity would, in general, have a higher mean amplitude than crosscorrelation functions for proximate geophones at some distance from the cavity.

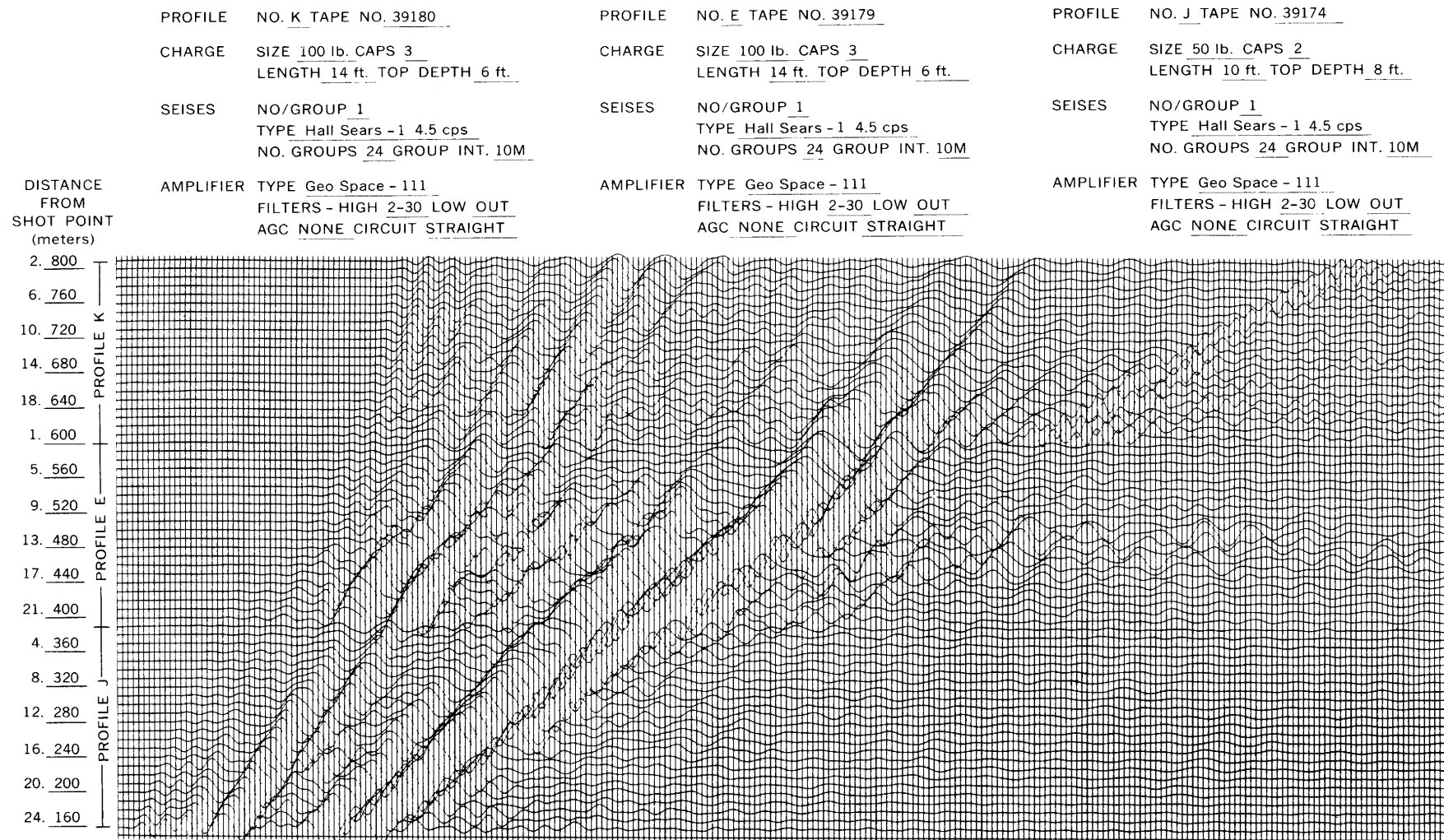


FIGURE 10.—Composite seismogram recorded at the U4B nuclear shot point, Nevada Test Site, from chemical explosions north of the seismic lines. Note the cavity oscillations recorded by seismometers over the cavity in the center spread (profile E). Timing lines are 0.010 seconds apart. Cps, cycles per second; INT., interval; AGC, automatic gain control.



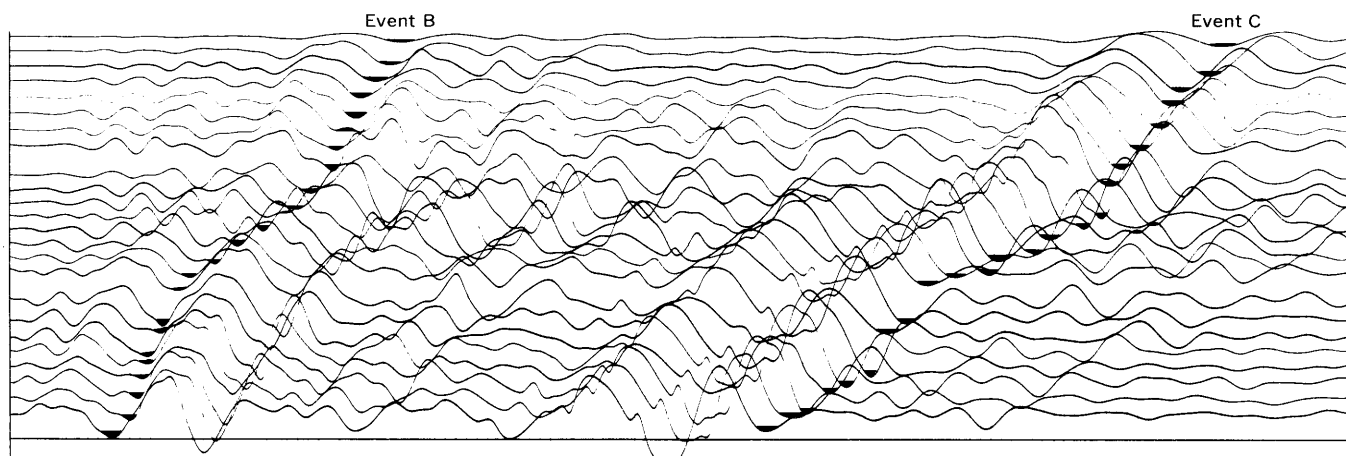


FIGURE 11.—Replay of tape 39179 showing delays in events B and C in the vicinity of the U4B shot point. A trough of each event has been darkened for emphasis.

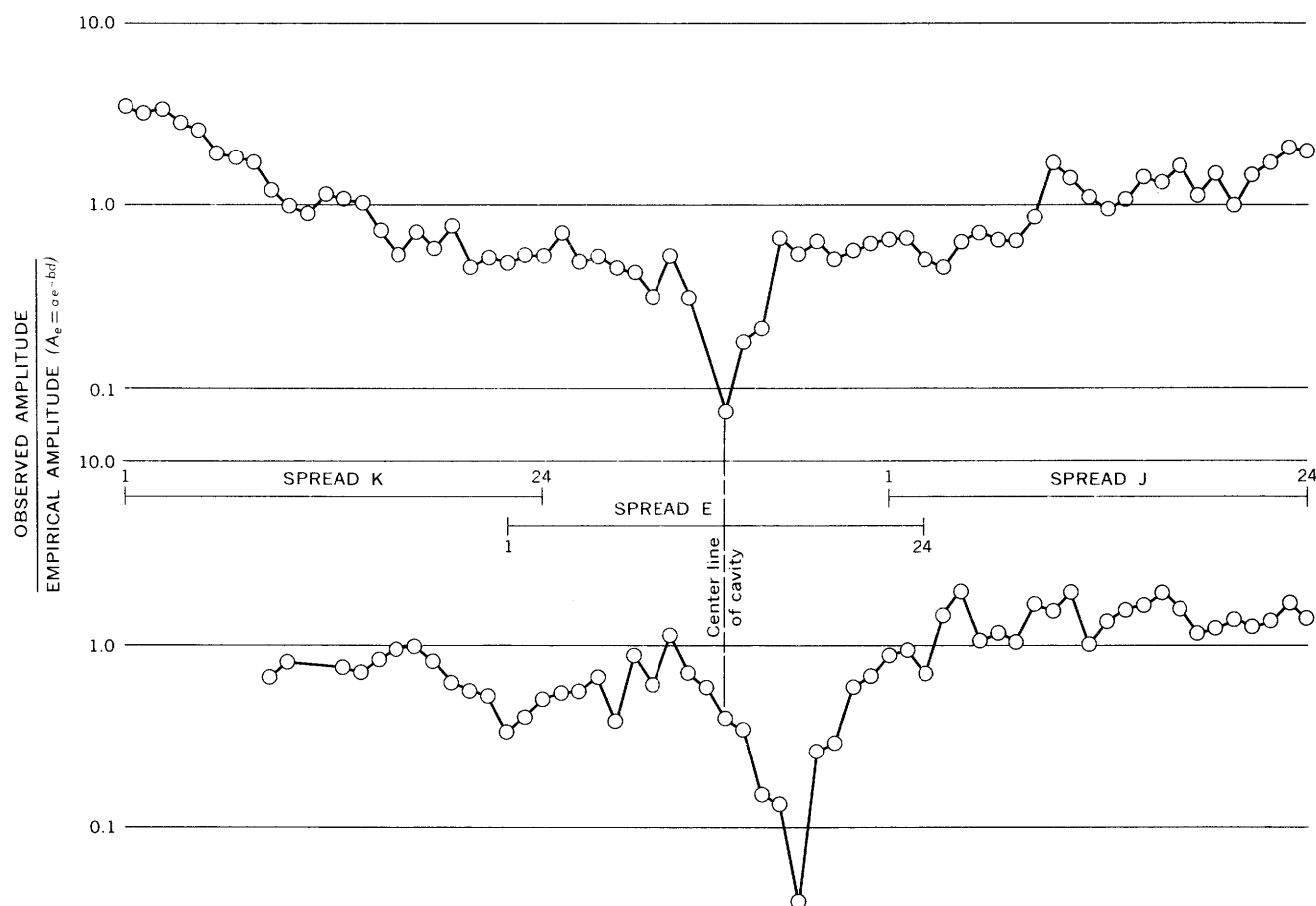


FIGURE 12.—Ratio of observed amplitudes of first-arriving seismic energy recorded in the vicinity of the U4B shot point to an empirical amplitude function,  $A_e = ae^{-bd}$ . Data in upper part of figure are from a shot north of the seismic lines; data in lower part of figure are from a shot south of the lines. Differences in shot-point locations cause asymmetry in amplitude anomalies.

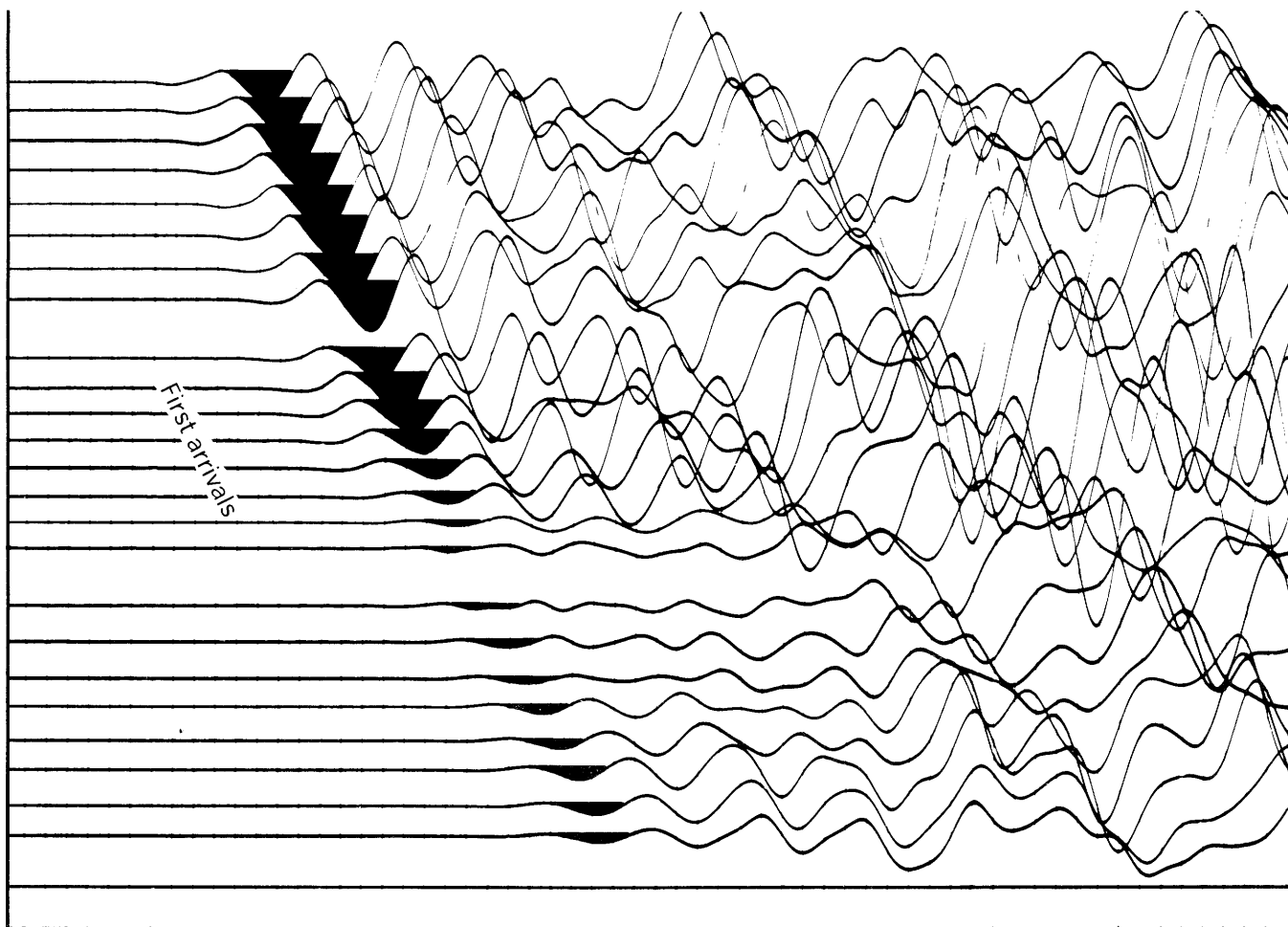


FIGURE 13.—Part of a seismogram recorded over the cavity at the U4B shot point showing attenuation of amplitudes of first-arriving energy from the south shot point.

To examine the potential usefulness of these three analytical methods, amplitude spectra were computed for all three sites, autocorrelation functions were computed for the U4B site and the Pisgah site, and the crosscorrelation function was computed for adjacent traces of the U4B site. Calculation of autocorrelation and crosscorrelation functions was significantly more time consuming and consequently more expensive on the computer than computation of amplitude spectra.

The crosscorrelation functions were not impressive, but both autocorrelation and spectra graphs were useful in the analysis of the data. Figure 14A is a graph of the spectrum as the function of frequency for selected traces from the Kana-a data, figure 14B shows the spectrum of selected traces from the U4B data, and figure 15 shows the autocorrelation function for selected traces from the Pisgah data. In figure 14, pronounced peaks appear in the spectra for

those geophones over and immediately adjacent to the cavities. The amplitude of the autocorrelation function is strikingly larger for those geophones over the Pisgah tunnel (fig. 15).

According to Biot's (1952) group-velocity curves (fig. 5), the following relation is approximately true for a cylindrical hole in an infinite solid:

$$D = \frac{V_s}{1.55f}$$

where  $D$ =diameter,  $V_s$ =shear-wave velocity, and  $f$ =resonant frequency.

Cavities at the test sites are not cylindrical holes in infinite solids, however, and some departures from theory can be expected. The Kana-a tunnel is open on one end where the roof has collapsed and extends perhaps 10 to 20 m into the ground before rubble fills it. The exact thickness of the roof material is not known but probably does not exceed 1 m in the area

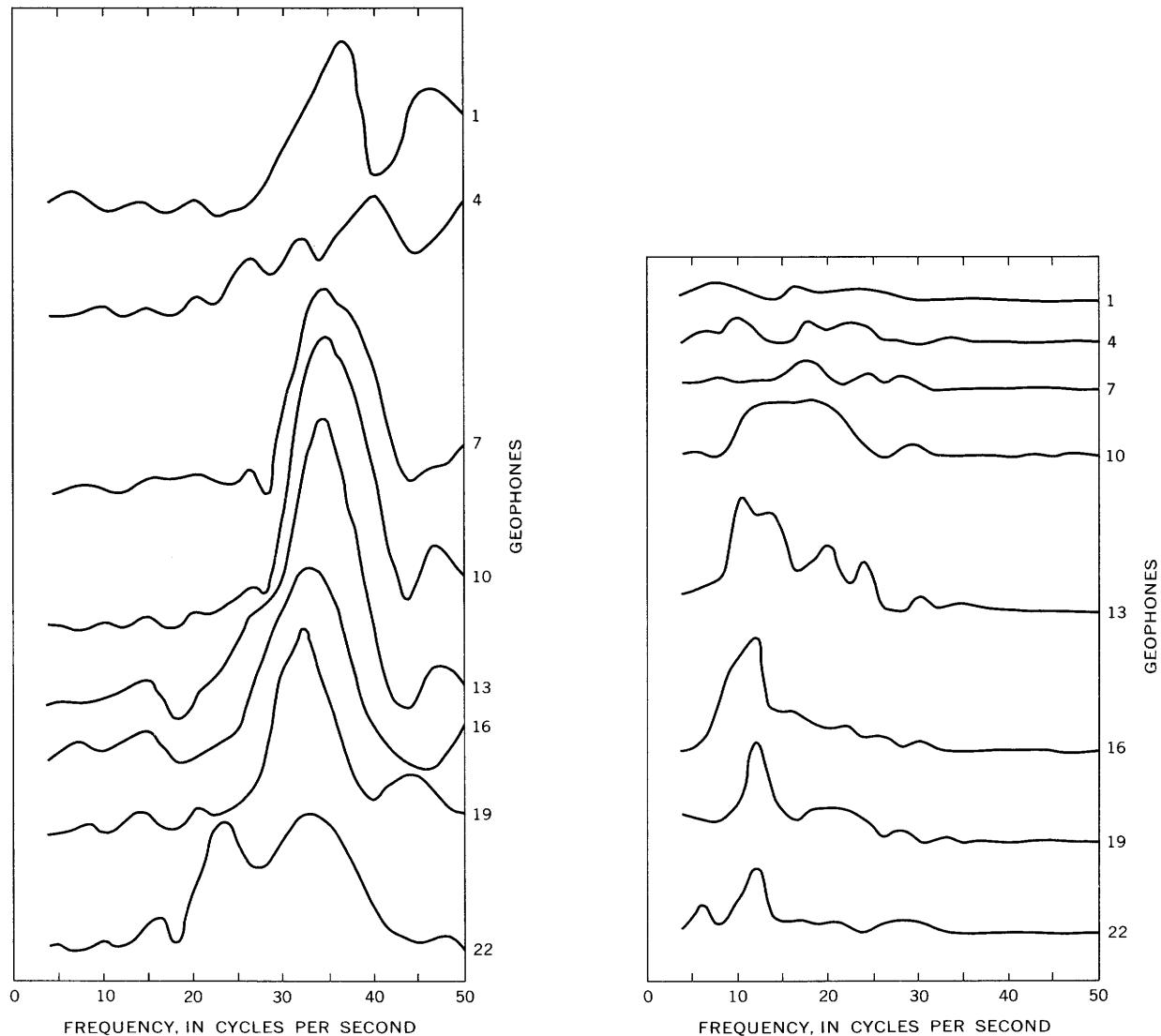


FIGURE 14.—Amplitude spectra calculated for selected seismic recordings. *A* (left), Over and adjacent to a lava tunnel in the Kana-a lava flow, Coconino County, Ariz. *B* (right), Over and above the U4B cavity at the Nevada Test Site.

where investigated. Radial dimensions of the Pisgah tunnel where crossed by the seismic lines range from about 3 to 10 m (see figs. 3, 8). The roof where investigated (profiles A and B) had an average thickness of about 2 to 3 m.

The U4B cavity is thought to be lens shaped with the upper surface convex upward. The shape of the lower surface has not been determined; nor has the diameter of the cavity been determined, although it is estimated to be at least 30 m (F. N. Houser, oral

commun., 1965). The thickness of the overburden is 25 m.

Table 1 summarizes data available on test-site materials. For the Kana-a and Pisgah sites, the calculated diameters exceed the maximum measured diameters by a factor of about 3. If the estimated 30 m is correct for the U4B diameter, then experimental data agree closely with the simplified theoretical calculations. Small errors are possible in the experimental data.  $V_s$  is probably accurate to within

15 percent for the Pisgah and U4B determinations, the Kana-a  $V_s$  determination, to within 2 or 3 percent. The dominant frequencies vary somewhat from detector to detector, and consequently a 5-percent error is probably possible in the determination of  $f$  for all sites.

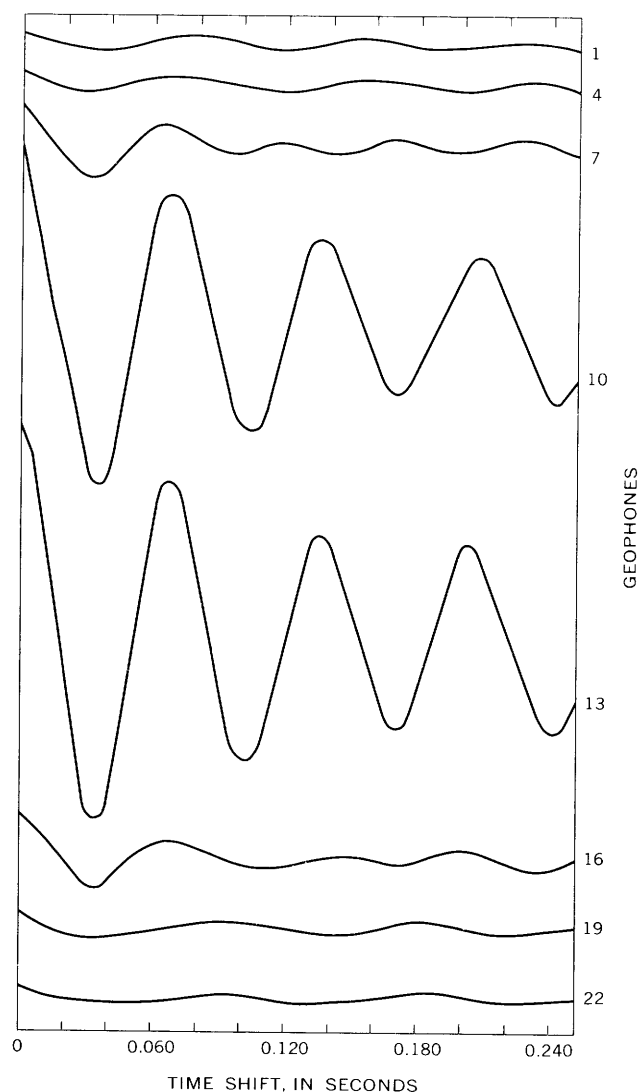


FIGURE 15.—Autocorrelation function for selected seismic recordings over and adjacent to Pisgah lava tunnel, San Bernardino County, Calif.

TABLE 1.—Cavity statistics

[ $V_p$ , compressional-wave velocity;  $V_s$ , shear-wave velocity;  $f$ , dominant frequency;  $D$ , maximum diameter of cavity]

Site	Rock	$V_p$ (mps)	$V_s$ (mps)	$f$ (cps)	$D$ (calculated in m)	$D$ (measured in m)
Kana-a	Basalt	800	450	34	8	2.5
Pisgah	Basalt	1,100	650	15	28	10
U4B	Alluvium	850	500	12	27	( <sup>2</sup> )

<sup>1</sup> Estimated to be 0.6 of compressional-wave velocity.

<sup>2</sup> Unknown; vertical dimension is 14 m, horizontal dimension estimated to be at least 30 m (F. N. Houser, oral commun., 1965).

### SUMMARY

Oscillations of relatively long duration and narrow bandwidth have been recorded over cavities in lava and alluvium at depths ranging from 1 to 14 m. They are probably radial oscillations of the cavity walls, and calculations show that dominant frequencies are generally within a factor of 3 of those computed by Biot (1952) for the radial oscillations of a cylindrical hole. Delays in arrival times and anomalous attenuation of seismic waves traversing cavities have also been recorded. Fractured and broken rock in the chimney is thought to be responsible for delays in the Rayleigh waves and possibly for trapped waves observed at the U4B cavity.

Fourier analysis and autocorrelation offer promise for detection of these and similar resonant seismic phenomena in noisy backgrounds; crosscorrelation of proximate traces was less successful for this purpose.

### REFERENCES

- Biot, M. A., 1952, Propagation of elastic waves in a cylindrical bore containing a fluid: *Jour. Appl. Physics*, v. 23, p. 997-1005.
- Cook, J. C., 1965, Seismic mapping of underground cavities using reflection amplitudes: *Geophysics*, v. 30, no. 4, p. 527-538.
- Jet Propulsion Laboratory, California Institute of Technology, 1966, Ranger IX photographs of the moon, cameras "A," "B," and "P": *Natl. Aeronautics and Space Adm. Spec. Pub.* 112.
- Watson, Kenneth, Murray, B. C., and Brown, H., 1961, The behavior of volatiles on the lunar surface: *Jour. Geophys. Research*, v. 66, no. 9, p. 3033-3045.







